Engineering Quantum Biosensors with Nanodiamonds

Caroline Brustoloni, Penn State University, Department of Electrical Engineering *SUNFEST Fellow*
Henry Shulevitz, University of Pennsylvania, Department of Electrical Engineering *Ph.D. Candidate*
Lee Bassett, University of Pennsylvania, Department of Electrical Engineering *Advisor*

***Abstract*— Because of their size, colloidal stability, room temperature quantum properties, and exceptional biocompatibility, nanodiamonds (ND) containing nitrogen-vacancy (NV) centers have many promising applications in quantum sensing, biolabeling, and nanomedicine. By conjugating nanodiamonds to various biomolecules, such as antibodies, therapeutics, and reporter particles, we can create a nano-sensing platform with simultaneous detection, diagnostic, and treatment capabilities. However, current methods of conjugating biomolecules to the nanodiamond surface have low yield and a high tendency of forming agglomerates. Here, we investigate ways to prevent nanodiamond agglomeration and increase conjugation yield by nanodiamond emulsions to increase the number of potential conjugation sites by a factor of 4 X.**

***Index Terms*—Agglomeration, Aggregate, Biosensor, Conjugation, Emulsion, Hemin, Functionalize, Nanodiamond**

I. Introduction

Nanodiamonds (NDs) harbor many exceptional qualities for biomedical sensing applications: nanoscale magnetic, electronic, temperature, and pH sensitivity; biocompatibility; long-term optical stability; and an optically addressable spin state. In particular, nanodiamonds with nitrogen-vacancy (NV) centers–the pairing of a nitrogen atom and lattice vacancy–harbor the ability to sense even slight variations in the external magnetic and electric field [1], which has positive implications for biological systems.

NV-center nanodiamonds exhibit near-surface quantum effects at room temperature. Moreover, we can use NV-center ND spin states for relaxometry; nonradiative intersystem crossing allows us to optically detect the NV center's spin state. Thus, we can utilize nanodiamonds in optical sensors to monitor ambient magnetic and electrical field changes.

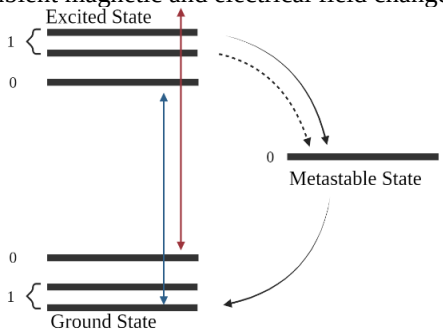

Figure 1. Nanodiamond states in relaxometry.

In biological systems, many cellular processes influence the magnetic and electric field, such as a change in the concentration of ions, nucleic acids, enzymes, etc. Monitoring the magnetic and electric field changes of these cellular processes has implications for disease diagnosis and treatment [2] by elucidating disease progression at the cellular level.

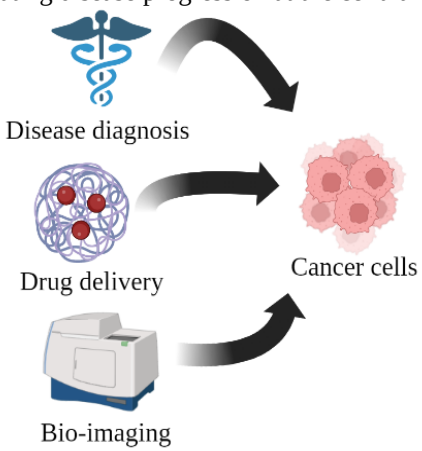

Figure 2. A nanomedicine application of nanodiamond sensors includes the detection, diagnosis, and treatment of cancer.

To utilize these NV-center nanodiamonds in biomedical sensors, we functionalize them with biomolecules. Biomolecules electrostatically attach to carboxyl groups on the surface of the nanodiamond. However, linking biomolecules to nanodiamonds involves a conjugation process that requires a low pH environment, which can cause the nanodiamonds to agglomerate due to exposed oxygen-containing functional groups on the surface [3]–a considerable drawback. Agglomeration negatively impacts the stability of the nanoparticles in solution, which leads to low dispersion rates and hinders their potential for use in medical applications [3].

In recent studies, researchers have attempted to functionalize nanodiamonds with biomolecules using various techniques. Bachman *et al.* functionalized diamond surfaces with TEMPO, a paramagnetic species, for use as a chemical detection scheme that harnesses the power of the NV quantum color defect [4]. This group achieved successful conjugation by utilizing radical-initiated grafting of ethynyl-terminated carboxylic acids to H-terminated diamond [4]. Akiel *et al.* used copper-free click chemistry to covalently attach DNA strands to ND surfaces that maintained the ability to undergo repeated hybridizations [5]. Yan *et al.* attached photosensitizer protoporphyrin (PpIX) to nanodiamond particles for use as both a contrast agent for magnetic resonance imaging and as a photosensitizer for photodynamic therapy for the diagnosis and treatment of cancer [6]. Though novel in their approaches and applications, these studies fail to directly address the problem of agglomeration.

In this study, we explore various methods of preventing agglomeration and increasing yield during the

conjugation of dye to nanodiamonds. We use dye in this study so we could use the color as a sign of successful conjugation, but we ultimately hope to replace the dye with proteins, antibodies, therapeutics, etc. We compare nanodiamonds emulsified with hemin at various ratios. Additionally, we investigate the role of a buffer in stabilizing the nanodiamond solution's pH and its optimal placement in the conjugation process.

To discern if agglomeration occurred, we determine the size of the particles in solution with dynamic light scattering (DLS). Dynamic light scattering also measures colloidal stability, another indicator of agglomeration. To gauge the yield and efficiency of the conjugation process, we determine the relative concentration of the particles before and after conjugation with ultraviolet-visible spectroscopy. Our optimized conjugation process results in less agglomeration, an increased conjugation yield, and four times increase in the number of potential conjugation sites.

II. Background

A. Hemin and Nanodiamond Emulsions

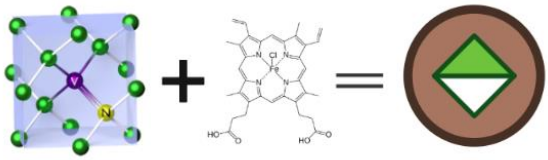

Figure 3. Hydrophobic nanodiamonds and hemin emulsified creates hemin-coated nanodiamonds.

We can functionalize nanodiamond surfaces with various biomolecules and therapeutics to customize them for use in disease diagnosis and treatment. We emulsify hydrophobic nanodiamonds with hydrophilic hemin. We choose hemin because it possesses a cage structure of carboxyl groups. Additionally, it does not emit any fluorescent emissions at an excitation of 532 nm—the excitation wavelength of the NDs. Creating an emulsion with NDs and hemin exposes more reactive surface carboxyl groups on the nanodiamonds. The emulsions also improve colloidal suspension and prevent agglomeration, allowing them to remain dispersed in solution for longer. We can then form covalent bonds between the carboxyl groups of the hemin and the amine groups of the conjugates—biomolecules, therapeutics, and markers—for in vivo and in vitro fluorescence imaging and drug delivery.

In our experiments, we compare the performance of these nanodiamond-hemin emulsions to aqueous carboxylated nanodiamond. We use carboxylated nanodiamonds because carboxyl functional groups offer an excellent basis for further surface modification. However, the nanodiamond-hemin emulsions should allow us to increase the number of carboxyl groups by a thousand-fold.

B. Nanodiamond Agglomeration

Many factors cause nanodiamond agglomeration; thus, avoiding agglomeration requires preventative measures at every step of the conjugation process.

Some innate nanodiamond agglomeration occurs due to oxygen-containing surface functional groups. We can prevent some of this aggregation by coating them with hemin, as previously mentioned.

In addition to the agglomeration of nanodiamonds that occurs naturally, an acidic environment can also cause these aggregates. The conjugation process of dye to nanodiamond requires the addition of 1-Ethyl-3-(3-dimethylaminopropyl) carbodiimide (EDC) and sulfonic acid, which significantly decreases the pH of the solution. Thus, we propose to maintain a higher pH with a buffer centered at a pH of 8 to prevent agglomeration.

Dialysis can also cause an increase in the presence of agglomeration of nanodiamond particles. We utilize dialysis as a separation technique to remove unwanted compounds from the solution through diffusion. We add hemin, EDC, sulfo-NHS, and dye superfluously to ensure an adequate supply for conjugation and remove the excess in this step. To reverse some of this inevitable agglomeration, we propose sonicating the solution at several intervals throughout dialysis.

III. Procedure

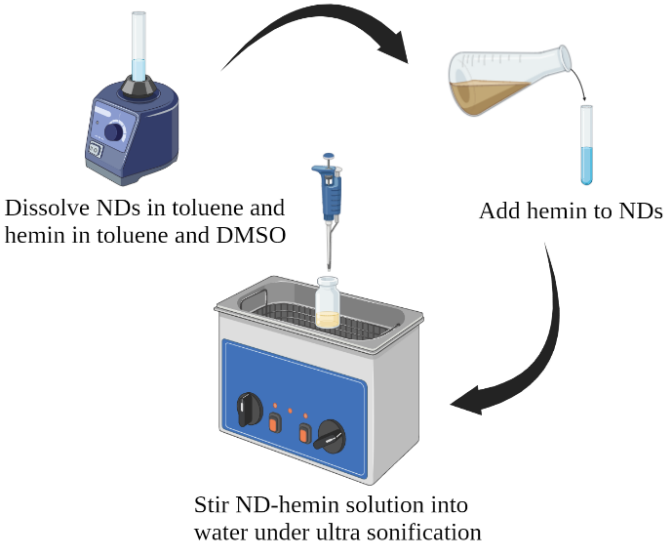

Figure 4. Procedure for creating nanodiamond-hemin emulsions.

A. Emulsifying Nanodiamond with Hemin

We prepare emulsions with 1:35k (10:1), 1:25k (15:1), and 1:18k (20:1) mole (mass) ratios of ND to hemin. For reference, a 1:1 mass ratio of ND to hemin approximately equals 360K hemin to 1 ND. We chose these ratios because approximately 25K hemin particles can coat a single nanodiamond surface.

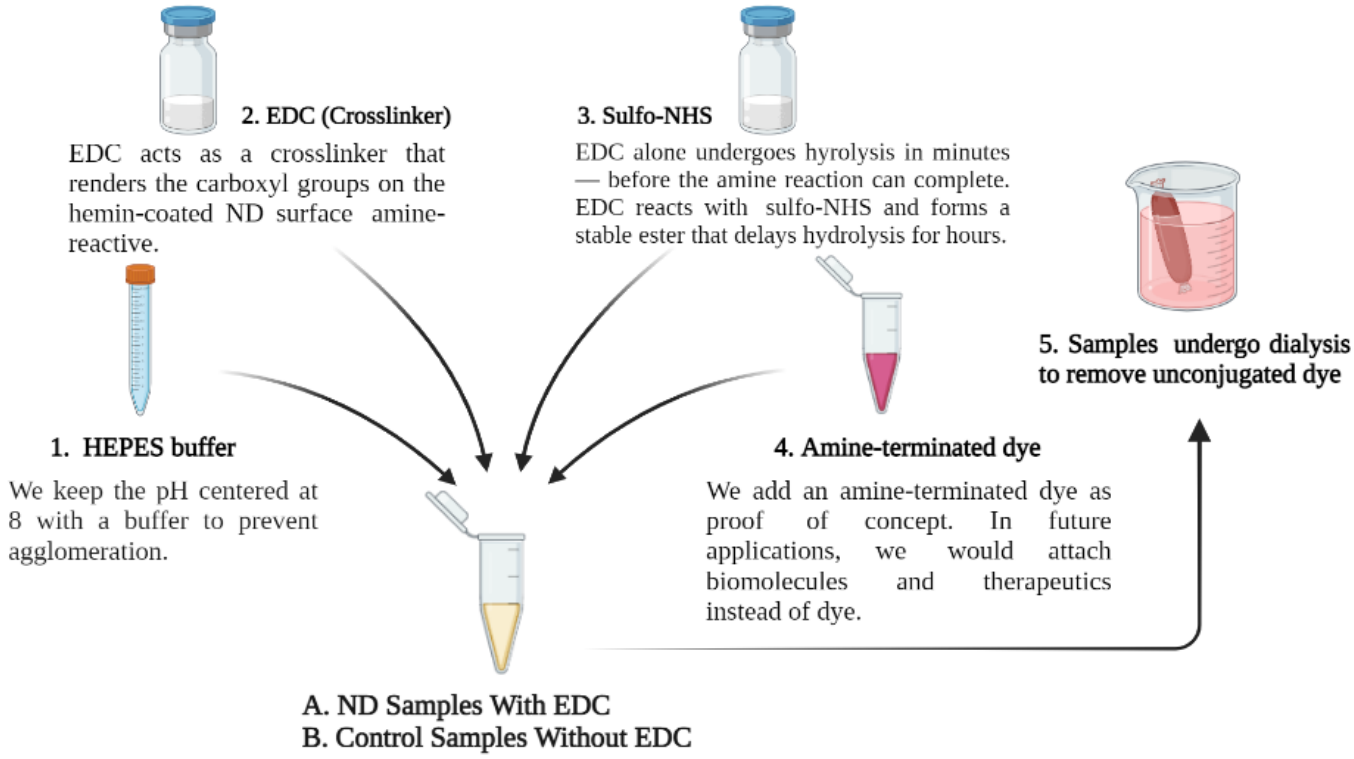

Figure 5. Conjugation process for attaching amine-terminated dye to nanodiamond surface.

For each sample, we dissolve 1 mg fluorescent NV-center nanodiamond in 60 uL of toluene via ultra-sonification. Toluene serves as a solvent for the nanodiamond. Before adding hemin to the nanodiamond solution, we first mix 3.6 mg of hemin into 1 mL of toluene and 100 uL of dimethyl sulfoxide (DMSO). DMSO enables the hemin-coated NDs to dissolve in water. Each nanodiamond solution sample receives a different quantity of the hemin solution to achieve the desired ratio of ND to hemin. To produce the emulsion, we manually stir the ND-hemin solution into 4 mL of water while simultaneously ultrasonicating the whole sample for 5 minutes. Then, we leave the emulsions uncapped overnight to let the toluene evaporate. Finally, we put the emulsions in dialysis to purify the samples of contaminants.

Before conjugation, we check the absorbance of the emulsions using ultraviolet-visible spectroscopy and the size of the particles. We later compare this data to the data collected after we conjugate the emulsions to dye.

B. *Conjugating Dye to Nanodiamond*

To conjugate dye to hemin-coated nanodiamonds, we induce amine reactions between the dye and the carboxyl groups on the nanodiamond surface with EDC and sulfo-NHS. While EDC alone hydrolyzes in minutes, sulfo-NHS delays this process for hours, enabling the conjugation process to complete successfully. We also experimented with adding HEPES or PBS as buffers to prevent agglomeration. In our final recipe, we use 35 uL HEPES, 1.5 mg EDC, and 1.6 mg of Sulfo-NHS. We let the conjugation process carry out on an incubator shaker at room temperature. Because light bleaches the dye, we protected the samples from ambient light by wrapping them with aluminum foil. As a final step, we put the samples in dialysis to remove any unconjugated dye.

IV. Experimental Results

A. *Nanodiamond-hemin emulsion characterization*

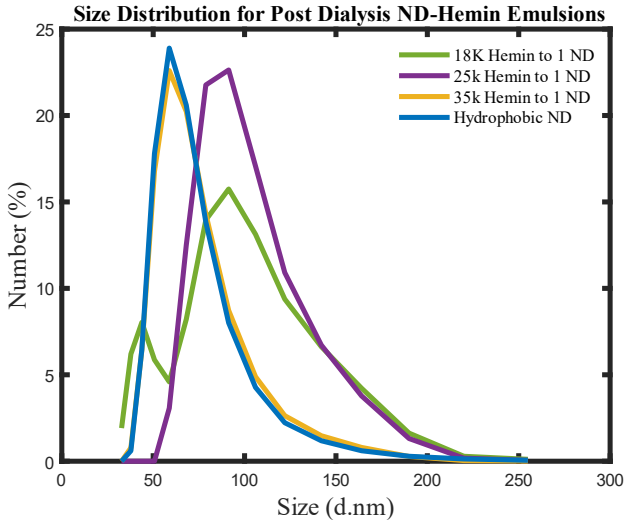

Figure 6. Size distribution for post-dialysis nanodiamond-hemin emulsions measured via dynamic light scattering.

We utilize dynamic light scattering to determine the size of the particles in the emulsions and of the hydrophobic nanodiamonds alone. In Fig. 6, we can see that a higher ratio of hemin to NDs leads to smaller particle size. It appears that more hemin creates single nanodiamond emulsions while too few hemin particles create multi-nanodiamond emulsions. We favor the single nanodiamond emulsions over the multi-nanodiamond emulsions because we want to avoid agglomeration.

Figure 7. Single nanodiamond emulsions compared to multi-nanodiamond emulsions.

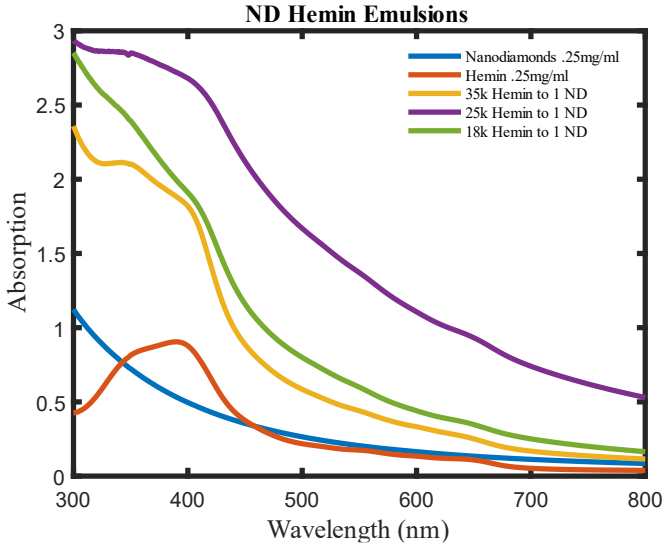

Figure 8. Absorption with respect to wavelength graph of nanodiamond-hemin emulsions measured via ultra-violet spectroscopy.

We use ultra-violet spectroscopy to measure the scattering and absorption characteristics of the nanodiamonds alone, the hemin alone, and the nanodiamond-diamond emulsions. Nanoparticle scattering takes the form of $\sim 1/\lambda^4$. Changes in the magnitude of these curves (increased scattering) after conjugation indicate agglomeration or the addition of materials that may have contaminated the sample.

B. *Investigating Agglomeration*

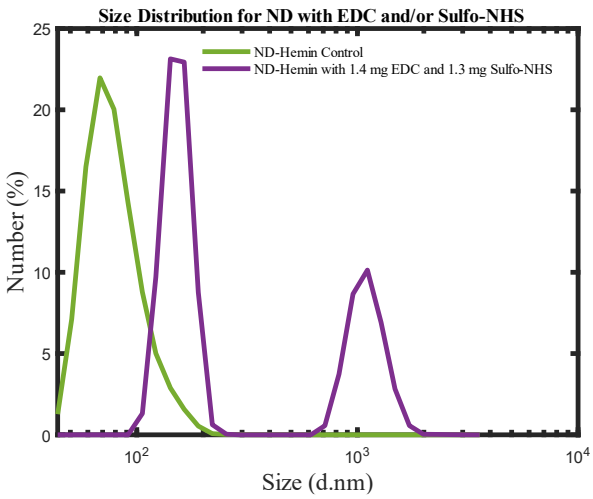

Figure 9. Size distribution of nanodiamonds with the addition of EDC and sulfo-NHS measured via dynamic light scattering.

We find that nanodiamonds agglomerated severely from the addition of EDC and sulfo-NHS. In Fig. 9, the nanodiamond-hemin emulsion with 1.4 mg of EDC and 1.3 mg of Sulfo-NHS has increased in size by a magnitude of 10. We conjecture that the dissociation of the reagents into acids causes this agglomeration.

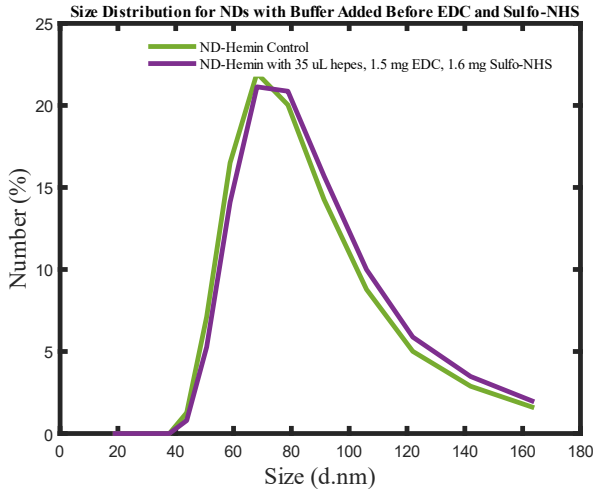

Figure 10. The distribution of nanodiamonds with the addition of HEPES buffer before EDC and sulfo-NHS measured via dynamic light scattering.

Adding HEPES buffer before EDC and Sulfo-NHS keeps the pH at 8 throughout the conjugation process, which prevents some agglomeration.

C. *Conjugated nanodiamond characterization*

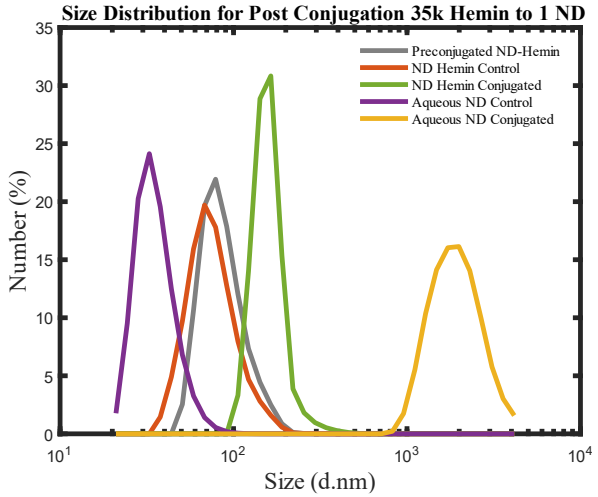

Figure 11. Size distribution of post conjugated nanodiamond-hemin emulsions and aqueous nanodiamond measured via dynamic light scattering.

During conjugation, the uncoated aqueous nanodiamonds agglomerate significantly. Although the conjugated nanodiamond-hemin emulsions increase in size, they remain a factor of ten smaller than the uncoated aqueous nanodiamonds. We can attribute some agglomeration of the nanodiamond-hemin emulsions to the instability of dye molecules. In general, it appears that coating nanodiamonds with hemins help prevent agglomeration because of the additional surface carboxyl groups.

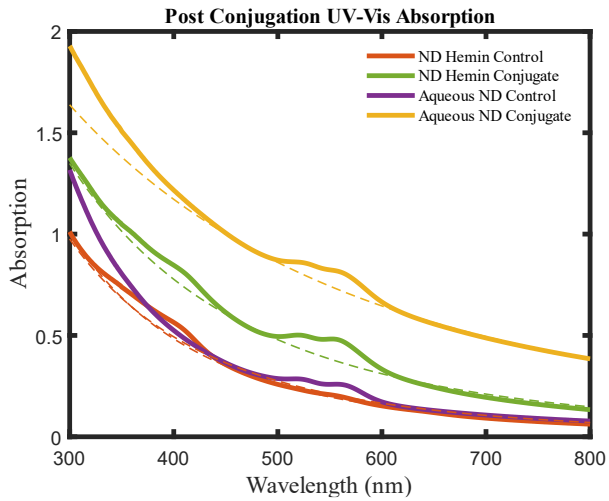

Figure 12. Absorption with respect to wavelength curves of the conjugated nanodiamond-hemin emulsions and aqueous nanodiamond measure via ultra-violet spectroscopy.

To determine the presence of dye, we compared the absorption curves of the conjugated nanodiamond-hemin emulsions and aqueous nanodiamond to nanodiamond scattering curves. Deviation from the scattering curves indicates the presence of the added dye.

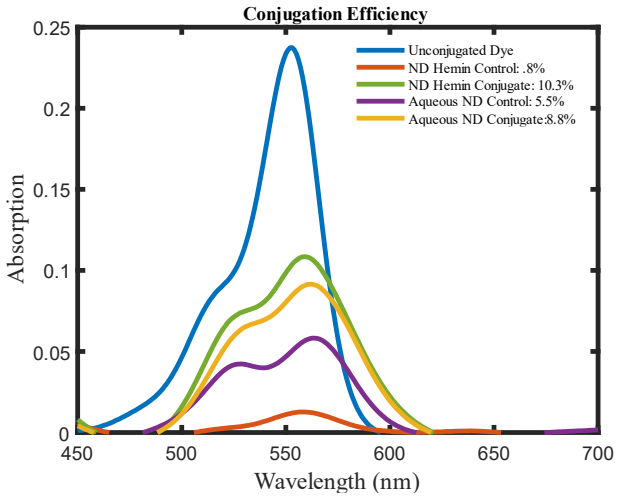

Figure 13. Difference between absorption of nanodiamond scattering curve and conjugated nanodiamond samples to determine conjugation efficiency.

To determine the efficiency of the conjugation process, we subtracted the nanodiamond scattering curves from the actual absorption curves to isolate the dye signal. By comparing to unconjugated dye, we can determine the efficiency of our process. We compare the integral of the difference between the scattering curve and the actual curve with the integral of the unconjugated dye curve. Using this method, we find that our conjugation process with the nanodiamond-hemin emulsions has a conjugation efficiency of 10.3% —higher than the control groups and the conjugated aqueous nanodiamond sample. In Fig. 13, the dye remaining in control samples indicates absorption to the ND surface.

V. Discussion and Conclusion

A. The persistence of agglomeration

When tracking the size of the nanodiamond clusters at every step of the conjugation process—from making the emulsion to adding the dye—it appears that agglomeration occurs at every step. However, the largest aggregates occur when we add EDC and sulfo-NHS. At this step, the nanoparticle clusters grow to thousands of nanometers in diameter. Agglomeration seems irreversible once it occurs, thus, we must take precautions to prevent it in every step of the conjugation process. By adding a buffer before the EDC and sulfo-NHS, the pH never plummets to an acidic level. Therefore, it never faces conditions that cause agglomeration.

Other factors that may contribute to agglomeration include loss of the coating material—hemin—during dialysis. Furthermore, the dye could be less stable than water. Possible solutions for agglomeration to investigate in the future includes increasing or modifying the emulsion material and utilizing more stable conjugate materials.

B. Further experimentation

Overall, we achieved 10.3% conjugation efficiency with our optimized conjugation process of adding 35 uL HEPES buffer, EDC, and Sulfo-NHS. To increase this conjugation efficiency, we may need to further characterize the conjugated samples. We could analyze them with Fourier-transform spectroscopy to confirm that covalent bonds formed between the ND-hemin emulsions and the conjugates. In further experiments, we could also attempt to emulsify the nanodiamonds with other materials—oleic acid or other porphyrin materials. Additionally, we could try to conjugate the emulsion to different biological materials—antibodies, proteins, and oligos—or charge or spin labels for enhanced sensing. Finally, we could perform *in vivo* or *in vitro* sensing experiments with the conjugated nanodiamonds in a clinical setting.

Acknowledgment

The authors would like to acknowledge the support of the National Science Foundation, through NSF REU grant no. 1062672. The authors would also like to thank Cherie R. Kagan, Andrew Tsourkas, Ahmad Amirshaghaghi, and Tzu-Yung Huang for their continuous support and guidance throughout this project.

References

[1] R. Schirhagl, K. Chang, M. Loretz, and C. L. Degen, "Nitrogen-vacancy centers in Diamond: Nanoscale Sensors for Physics and Biology," *Annual Review of Physical Chemistry*, vol. 65, no. 1, pp. 83–105, 2014. USA: Abbrev. of Publisher, year, ch. *x*, sec. *x*, pp. *xxx–xxx.*

[2] B. Cuffari, "Nano diamond biosensors to monitor intracellular processes," *AZoNano.com*, 24-Mar-2017. [Online]. Available: https://www.azonano.com/article.aspx?ArticleID=4439#:~:text=Nanodiamonds%20(NDs)%20are%20diamond%20particles,and%20tunable%20surface%20structures1. [Accessed: 17-Jun-2022].

[3] J.-X. Qin, X.-G. Yang, C.-F. Lv, Y.-Z. Li, K.-K. Liu, J.-H. Zang, X. Yang, L. Dong, and C.-X. Shan, "Nanodiamonds: Synthesis, properties, and applications in Nanomedicine," *Materials & Design*, vol. 210, p. 110091, 2021.

[4] B. F. Bachman, Z. R. Jones, G. R. Jaffe, J. Salman, R. Wambold, Z. Yu, J. T. Choy, S. J. Kolkowitz, M. A. Eriksson, M. A. Kats, and R. J. Hamers, "High-density covalent grafting of spin-active molecular moieties to Diamond Surfaces," *Langmuir*, vol. 37, no. 30, pp. 9222–9231, 2021.

[5] R. D. Akiel, X. Zhang, C. Abeywardana, V. Stepanov, P. Z. Qin, and S. Takahashi, "Investigating functional DNA grafted on nanodiamond surface using site-directed spin labeling and electron paramagnetic resonance spectroscopy," *The Journal of Physical Chemistry B*, vol. 120, no. 17, pp. 4003–4008, 2016.

[6] L. Yan, A. Amirshaghaghi, D. Huang, J. Miller, J. M. Stein, T. M. Busch, Z. Cheng, and A. Tsourkas, "Protoporphyrin IX (ppix)-coated superparamagnetic iron oxide nanoparticle (Spion) nanoclusters for Magnetic Resonance Imaging and Photodynamic therapy," *Advanced Functional Materials*, vol. 28, no. 16, p. 1707030, 2018.